Contents lists available at ScienceDirect

Computer Networks

Coordinated multi-cell cooperation with user centric dynamic coordination station

Baha Uddin Kazi, Gabriel Wainer*

Department of Systems and Computer Engineering, Carleton University, Ottawa, ON, Canada

ARTICLE INFO

ABSTRACT

Existing cellular wireless networks are facing fundamental challenges due to the exponential demand of mobile data traffic, the need of higher data rates, user coverage, lowering latency, and minimizing signaling overhead. In order to address these challenges, future cellular networks will require adopting a multi-cell multi-tier cooperative architecture. However, in multi-cell cooperation, the user equipment (UE) needs to estimate the channel state information (CSI) and feed it back to the base station (BS) scheduler for adaptive resource management. This results in a significant increase of signaling overhead and feedback latency into the cooperative networks. These overhead and latency are the two key challenges to achieve gains in coordinated multi-point (CoMP) operation. In this research, we study the control plane protocols for cooperative communications and propose a novel coordination architecture to improve the performance of multi-cell cooperative cellular networks. We examine the performance of the proposed CoMP coordination architecture by performing simulation on different homogeneous and heterogeneous scenarios. Simulations outcome of the multicell cooperative cellular networks show that the proposed coordination architecture has the potential to reduce the signaling overhead and feedback latency compared to conventional methods that eventually will improve the performance of cooperative cellular networks.

© 2019 Elsevier B.V. All rights reserved.

1. Introduction

The ongoing social development and arrival of new applications proliferate the demand of immense data traffic and services in wireless cellular networks. The number of mobile broadband subscribers is expected to reach 7.7 billion by 2021 and mobile data traffic is expected to reach 48.3 Exabytes per month by 2021 [1,2]. Moreover, the 5G and beyond wireless cellular networks also consider potential use cases, such as autonomous vehicle control, smart cities, remote surgery, tactile internet etc. Due to these issues, 5G networks are expected to support an enormous number of connected devices, high bandwidth, being ultra-high reliable, ultra-low latency, minimum signaling overhead, energy efficient, and almost with 100% coverage [3,4]. Therefore, to keep the user experience at a satisfactory level by achieving the above goals, we need to provide new cellular algorithms and technologies.

In this context, network densification such as ultra-dense networks (UDN) and ultra-dense heterogeneous networks (UDHetNet) are considered as the foundation to achieve the data traffic growth needed [5–7]. Nevertheless, in ultra-dense networks, inter-cell in-

terference (ICI) is high due to the dense deployment of small cells, and the randomness of the network topology [8]. Thus, this dense deployment of the networks needs advanced interference mitigation techniques in order to coordinate, cancel or exploit such interference. Multi-cell cooperation or coordinated multipoint (CoMP) transmission and reception is considered as an effective method for mitigating inter-cell interference [9–11]. The idea of CoMP is to evolve from the conventional single-cell multi-user system to a multi-cell multi-user system, so that the UEs close to the cell edge can be served by multiple base stations. In CoMP-enabled systems, the base stations (BS, also called evolved Node B – eNB) are grouped into cooperating set. The eNBs of each of these cooperating sets exchange information among them, and they process signals and provide services to the users jointly. As a result, the UEs can receive their signals simultaneously from one or more transmission points in a coordinated or joint-processing method, which can improve data rate coverage and cell edge throughput [12,13].

However, in CoMP enabled networks, the scheduler needs accurate and updated channel state information (CSI) for adaptive transmission, as well as appropriate radio resource management (RRM) [12,14]. In order to provide this information to the scheduler, the UEs estimate the CSI and report it to their serving eNB periodically. The cooperating eNBs exchange the received CSI and/or

* Corresponding author.
    E-mail addresses: bahauddinkazi@sce.carleton.ca (B.U. Kazi), gwainer@sce.carleton.ca (G. Wainer).

data among them providing services to the UE. Accordingly, the CSI feedbacks increase the signaling overhead into the networks significantly that requires high bandwidth backhaul [12,13,15]. Therefore, signaling overhead depends on the CoMP coordination architecture. There are two types of control architectures available in the literature: *centralized* and *distributed* [16–18]. In the centralized architecture, a central unit is responsible for handling radio resource scheduling by processing the CSI feedback information from the UEs. On the other hand, in the distributed architecture, the coordinated cells exchange data and CSI over a fully meshed signaling network using X2 interfaces and a star-like S1 network. The X2 interface between two eNBs is used to exchange information such as CSI, scheduling information etc. in the cooperative communication. On the other hand, eNBs connect to the EPC (evolve packet core) using S1 interface. Both of the architectures increase signaling overhead significantly. We will discuss more details about the both of the architectures in Section 2. These signaling overhead and latency are the key causes for performance degradation of cooperative cellular networks [17,9].

The objective of this research is to develop new CSI feedback algorithms for minimizing the signaling overhead and feedback latency. We present a user-centric CoMP coordination architecture named *Direct CSI-feedback to Elected Coordination-station (DCEC)* [19–21], in which one of the cooperating eNBs in the CoMP cooperating set, elected dynamically, will act as a coordination station (CS), and the UEs in the cell edge within the same cooperating set will send the CSI feedback to this CS only. Thereon, the CS will analyze the received CSI information and will be in charge of scheduling. A cooperating set is a set of eNBs and RRHs that serve the UEs jointly [22]. In Section 3 we discussed the details of the CS election process. We also extended the control architecture for heterogeneous cellular networks named *DCEC-HetNet*.

In order to analyze the performance of the DCEC control architecture, we built a model and ran simulations of various scenarios suggested by the 3GPP specifications. Our simulation results show that DCEC reduces the number of control messages transmitted within the CoMP cooperating networks and their feedback latency. Though it requires more control messages to elect the CS in the startup transient period, under steady state it outperforms the other two architectures.

The rest of the paper is organized as follows: in Section 2, state of the art and related works that have been done in the same area are reviewed briefly. We present the DCEC control architecture for homogeneous multicell cooperative cellular networks in Section 3. In this section, we also present the extended DCEC approach for heterogeneous cellular networks named DCEC-HetNet. The CSI feedback schemes and the overhead models are presented in the Section 4. Simulation scenarios and results are presented in Section 5. Finally, we conclude in section 6.

2. Background and state of the art

The advances in wireless technologies and radio spectral efficiency as well as the demand of data rate, mobility and coverage lead to the development of the cellular networks. The next generation, 5G, is intended to overcome the challenges of existing cellular systems, such as the exponential growth of data traffic, coverage, latency, signaling overhead, energy consumption, and cost. 5 G networks are expected to provide approximately a system capacity of 1000 times higher, data rates 10 times higher, 25 times the average cell throughput, 5 times reduced latency and 10 times longer battery life when compared to the 4G networks [23,24]. To achieve these goals, 5G networks will adopt new technologies.

Network densification using small cells or dense heterogeneous networks (HetNets) is considered as an effective method to improve the capacity of cellular networks [25–27]. HetNets or ultra-
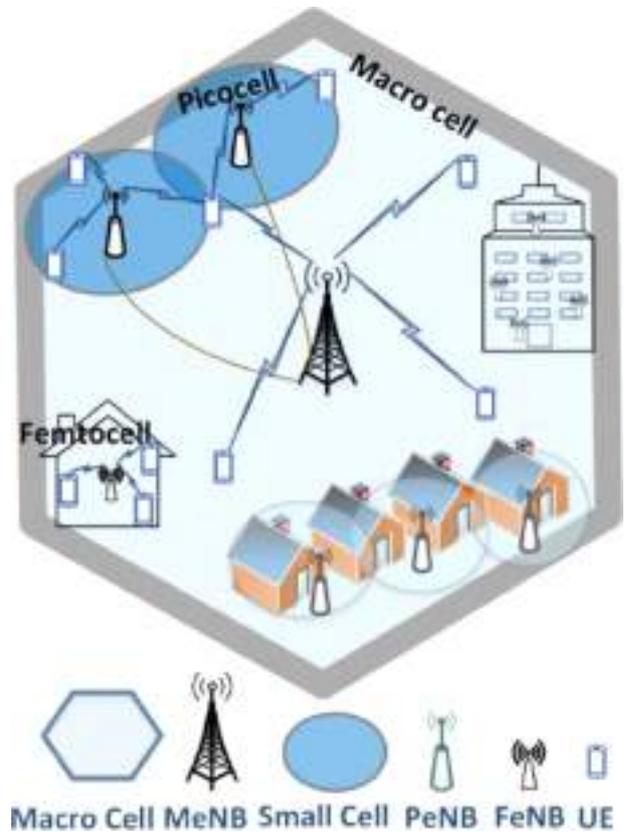

Fig. 1. Simplified architecture of dense heterogeneous cellular networks.

dense HetNets (UDHetNets) consist of coexisting macro-cells and low power nodes for small cells such as picocells, femtocells and remote radio head (RRH). The RRHs are mounted outside the macro base station and are connected to the eNBs or the BBU pool via optical fiber. RRHs do not have a baseband unit (BBU), and the central macro eNB (MeNB) or BBU pool is in charge of the control and the baseband signal processing. Pico eNBs are operator-installed low-power nodes with the same backhaul and access features as the macro eNBs. The typical transmit power range of a pico eNB is 23–30 dBm [28]. Home eNBs are low power user deployed access points. The typical transmit power of the HeNB is less than 23 dBm and the coverage area is considered less than 50 m [28].

Fig. 1 shows the overall architecture of a dense heterogeneous cellular network. As the size of the cells decreases, the number of cells will increase, providing service to more users with a better signal quality. Therefore, these low power small cells can reduce the load of the macrocells and increase the user coverage. However, the densification of cells can increase the interference and signaling load of the network [29].

3GPP, as well as other research communities, considered cooperative communications as one of the state-of-the-art techniques for the future wireless cellular networks [9,8]. Several research works focus on massive MIMO (multiple inputs multiple outputs), network densification with small cells or heterogeneous networks and multi-cell cooperation [3,9,22,26]. The basic idea of cooperative communications is to evolve the conventional single-cell multiple UEs system structure to multi-cell multiple UEs networks. This technique is known as coordinated multi-point (CoMP) transmission and reception. CoMP boosted up the cell-edge user's throughput by reducing the inter-cell interference. In CoMP, eNBs (base stations) are grouped into cooperating sets that exchange information and process signals and provide services to the users
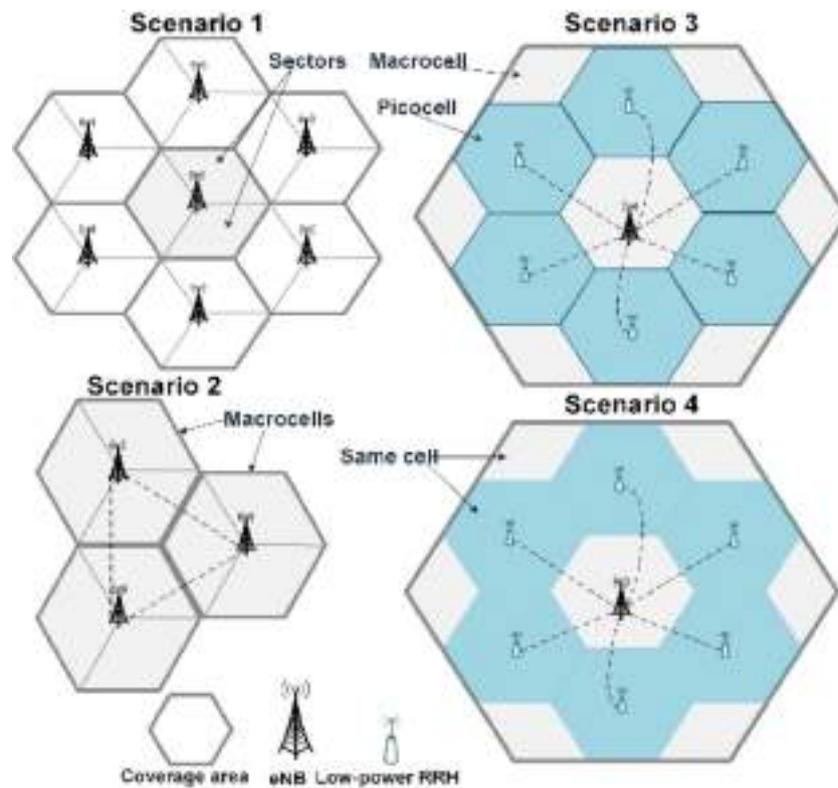
Fig. 2. CoMP scenarios suggested by 3GPP.

jointly. As a result, CoMP enables UEs to receive signals simultaneously from one or more transmission point in a coordinated or joint-processing method [12,13].

Fig. 2 shows different scenario for CoMP cooperation suggested by 3GPP [22,30]. In this figure scenario 1 shows an intra-site CoMP homogeneous macro network, and scenario 2 shows an inter-site CoMP homogeneous macro network. Scenario 3 and 4 show heterogeneous networks for CoMP cooperation. For heterogeneous networks, two layers of cells are used: one with high-power macro eNBs (MeNBs) and another with low-power RRHs. The low power RRHs do not have a baseband unit (BBU). The connection between the RRHs and the central macro eNB is considered optical fiber in LTE Release 11. The difference between them is that in Scenario 3, each RRH has a distinct cell ID, while in scenario 4 RRHs share the same cell ID with the associated MeNB [12,22].

The coordination architecture of CoMP cooperation can be defined as the way in which participating cell sites coordinate with each other to handle interference and scheduling when serving the UEs. A decentralized approach is proposed in [17] for multi-cell cooperative networks. In this approach, each UE directly feeds back its CSI to all collaborating eNBs. Liu et al. in [31], presented a novel media access control (MAC) protocol named CoopMAC for cooperation among the station in a wireless LAN. They also introduce opportunity cost and actual cost for helper station. The paper in [32], did performance analysis of a hybrid relaying protocol named RelaySpot for wireless networks. RelaySpot also consider cooperation at MAC layer of wireless network. In [33], the authors presented a centralized MAC approach for CoMP joint transmission. In this approach, the base stations are grouped into clusters. Within a cluster, one of the cells is preconfigured as the head sector, and the others act as proxies. The authors in [34] proposed a distributed architecture over an IP backhaul network between the eNBs for CoMP Joint Transmission (JT). Gao et al. proposed a modified version for dynamic cell selection for CoMP transmis-

sion. They extended the dynamic cell selection method to a Multi-Cell scenario, which originally is limited to one chosen transmission cell [35]. The paper in [36] studies the performance analysis of the CoMP joint processing (JP) transmission in the HetNets scenarios. Geirhofer and Gaal discuss CoMP for different HetNets scenarios in [37]. The authors also analyze the CoMP schemes and the deployment scenarios as well as the benefits and drawbacks of them. Hajisami and Dario [38], proposed Cloud-CFFR to increase the system spectral efficiency. This approach dynamically changes sub-band boundaries based on the number of active uses. In [39], authors proposed dynamic joint processing (DJP) to reduce inter and intra-cluster interference in CoMP. In this approach UEs are categories into low-mobility and high-mobility groups and based on that two coexisting clustering approaches are presented.

According to the literature, there are two types of coordination architectures available for CoMP transmission and reception: centralized and distributed [16–18] as we mentioned before. Fig. 3(a) shows the *centralized architecture*, in this architecture a central unit (CU) is responsible for radio resource scheduling by centrally processing the channel state information (CSI) feedback information from the UEs in the cell edge area of different cells within the cluster. The UEs estimate the channel state information related to all the eNBs and the low power nodes in the cluster and send it back to their serving eNBs. Then the serving eNB forwards the received CSI to the CU. Finally, the CU process the CSI and sends it back to the eNBs within the CoMP cooperation set. The CSI is exchanged among the coordinated eNBs through the X2 interface. The latency of the X2 interface is about 10 ms [40,41]. Therefore, this architecture suffers from signaling overheads and increases the feedback latency. Fig. 3(b) shows the *distributed architecture*. In this architecture, the UEs estimate the CSI related to all the cooperating eNBs and send it back to the corresponding serving eNBs. After receiving the channel state information from the UE, cooperating eNBs exchange the CSI among themselves over a fully meshed signal-
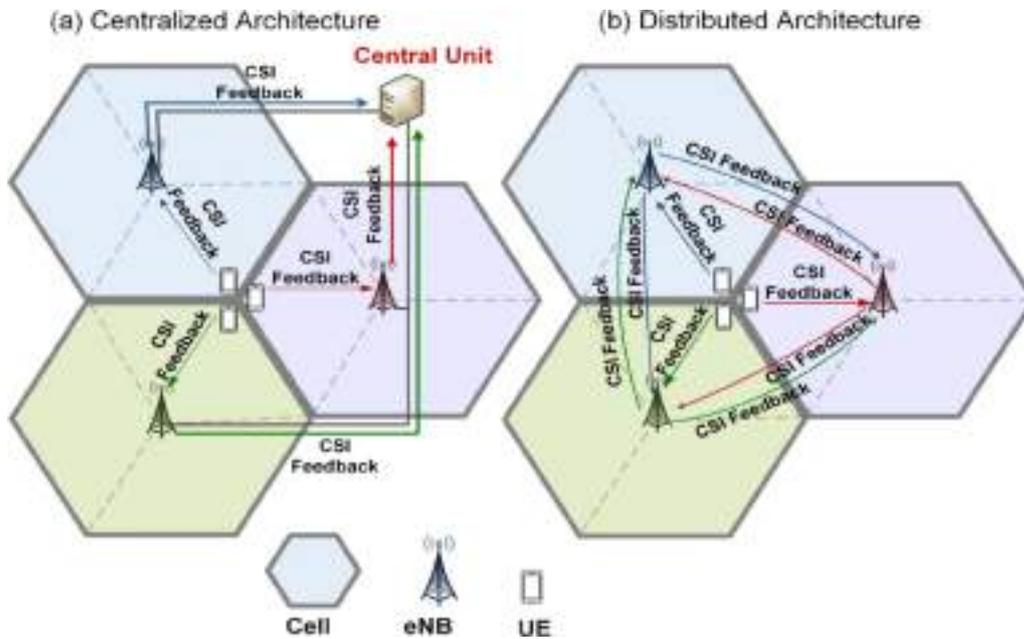
Fig. 3. Standard CoMP Control Architectures.

ing network using X2 interfaces. Based on the acquired CSI, coordinated eNBs schedule the resources independently. This architecture also increases the signaling overhead into the cooperative network with the increase of the number of eNBs into the cooperating sets [17,21].

The paper in [42] investigated the influence of CSI feedback delay on the throughput of MIMO systems. They also showed that the increase of the feedback delay causes the loss of the system throughput. The authors in [11] study the performance of CoMP joint transmission in ultra-dense networks (UDNs). They also focus on how to improve per area spectral efficiency in UDNs based on CoMP transmission. Liu et al. [8] show the performance of CoMP joint transmission and coordinated scheduling/beamforming from three different aspects with limited backhaul capacity. They did an analysis of CoMP performance in user's perspective, access point's perspective and network perspective. 3GPP discussed different deployment scenarios and challenges of small cell enhancements [25,43].

In this research, we study the control plane architecture for multi-cell cooperative communication and proposed new coordination architecture to overcome the challenges discussed before. We modeled the DCEC control architecture, a centralized and a distributed control architecture using the discrete event system specifications (DEVS) formalism [44,45], a formal modeling and simulation methodology for discrete-event dynamic systems. In the next section, we will discuss the DCEC CoMP coordination architecture in details for future cellular networks.

3. DCEC for future wireless cellular networks

As mentioned earlier, the coordinated multipoint (CoMP) transmission and reception can improve system performance, especially on the cell edges [12,9]. CoMP enabled networks require accurate and updated channel state information (CSI) at the scheduler for adaptive transmission and appropriate radio resource management (RRM) [12,14]. In order to do so, the UEs estimate the CSI and report it to their serving eNBs periodically. The serving eNB forwards this CSI to the scheduler. Consequently, it increases the CSI feedback overhead or the signaling overhead into the network significantly [15,13,12], with direct impact on the system's perfor-

mance [12]. This overhead depends on the CoMP coordination architecture. Existing CoMP coordination architectures (centralized and distributed) suffer of signaling overheads and increase the CSI feedback latency, as we discussed in the previous sections.

We present a new CoMP coordination architecture named Direct CSI-feedback to Elected Coordination-station (DCEC) [19,20], which intends reducing the signaling overhead and latency of the CSI feedback, increasing the throughput of the network [19]. Consider the users equipment in the cell edge area UEi, where $i=\{1, 2, …, n\}$. The UEi will send the CSI feed back to its serving eNB. The serving eNB will calculates the cooperating set {eNB1, eNB2, …, eNBm} to serve the UE jointly. One of the eNBs in the cooperating set will dynamically elect as a coordination station (CS) for a UE. Fig. 4 shows the signaling procedure of the DCEC scheme for homogeneous cellular networks to elect the CS. As an example, in this figure, the UE1 sends the CSI feedback to MeNB1 (serving eNB of the UE1). After receiving the CSI, MeNB1 calculates the cooperating set for the UE. To calculate this cooperating set, the serving MeNB (MeNB1 for UE1 in this example) compare the channel quality from the received CSI based on the predefined CoMP threshold (3dB-9 dB [46–48]). That is, if $RSRP_{max} - RSRP_{eNB_i} \leq CoMP_{Th}$, the eNB_i is included into the cooperating set. Where, $RSRP_{max}$ is the maximum received power and $CoMP_{Th}$ is the predefined CoMP threshold value. If the cooperating set contains more than one MeNB, then the serving MeNB (MeNB1) initiates the election algorithm by sending a CoMP request message to the other MeNBs in the cooperating set (MeNB2, MeNB3 in this case), including its own cell throughput. After receiving the CoMP request, they check their own resources and compare the received throughput with their own.

Based on the availability of resources, they send back a *request grant/reject* message, including the highest throughput and the CS id. After receiving the responses, the serving MeNB finds the CS based on the highest throughput and it notifies that to the other MeNBs within the cooperating set, and it sends the CoMP command to the UE (UE1). The UE replies an *ACK* message and switches to the CoMP mode. After establishing CoMP with the CS, the UEs send the CSI feedback only to the CS.

Each of the UEs in the cell edge area will go through the same process and UEs in the same CoMP cooperation set send the CSI
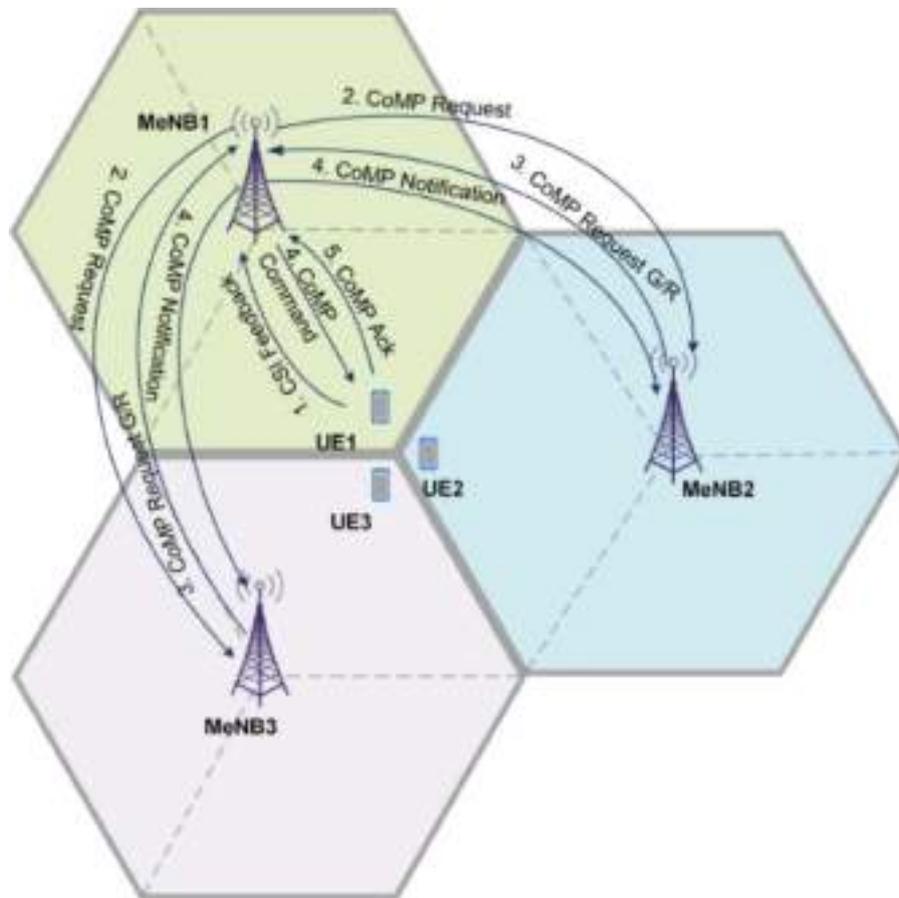
Fig. 4. Message transfer to establish CoMP with CS election in DCEC.

feedback to the CS only. All the UEs in the same CoMP cooperating set send the CSI feedback directly to the same CS. Thereon, the CS will analyze the received CSI information and will be in charge of scheduling. Therefore, the CSI feedback does not need to travel additional X2, S1 or fiber channels when the UE is in the CoMP cooperation set, which results in avoiding the extra latency of the CSI feedback transmission as well as reducing the signaling overhead into the network. Moreover, CS will also determine the cooperating set if any changes happened in the cooperation set, when the UE is in the CoMP service. The whole idea of the DCEC coordination architecture is shown in Fig. 5. For example, in this figure eNB1 is elected as the CS for UE2, UE3 and UE5. All the three UEs have the same cooperating set {eNB1, eNB2, eNB3}. Therefore, after the CS has been elected all of the three UEs send CSI feedback message to the CS (eNB1) only instead of sending their own serving eNB. Latency and overhead are inversely related to the throughput of the network, in particular for the coordinated schemes. However, if the feedback latency of the cooperating network is greater than the CSI feedback periodicity, then the scheduler will receive an outdated CSI [49]. As shown in [50,51], the throughput of the cell can increase by as much as 5% if the latency is reduced by 1 ms.

The algorithm to elect the coordination station in DCEC CoMP control architecture for homogeneous cellular networks is presented in the next subsection.

3.1. Coordination station election algorithm for DCEC in homogeneous cellular networks

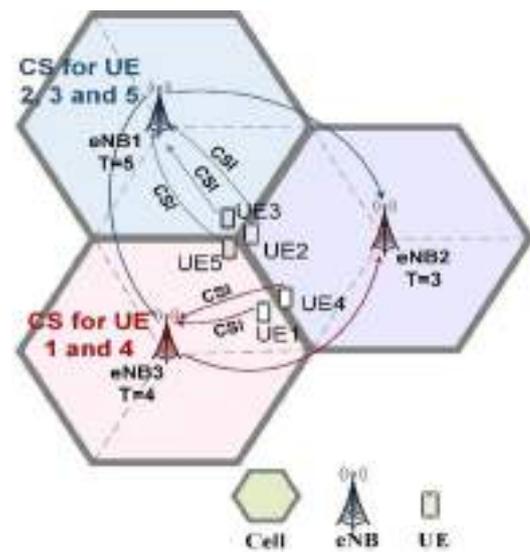To elect a Coordination Station (CS) dynamically, we use the following algorithm:

Fig. 5. Simplified view of the DCEC CoMP coordination architecture.

1. UE_i estimates the CSI and sends it to the serving $MeNB_i$.
2. Serving $MeNB_i$ receives the CSI Feedback and it calculates the CoMP cooperating set for UE_i.
3. If a CoMP cooperating set contains more than one MeNBs, the serving $MeNB_i$ declares itself as a CS
4. The declared CS sends a CS-Declaration message to other MeNBs in the cooperating set of UE_i

5. After receiving the message, other MeNBs in the cooperating set compare their throughput with the received CS throughput.
   a. If the received CS throughput is higher than the recipient's throughput (or the current):
      i. The CS ID will change to the received ID.
      ii. The recipient forwards the new CS information to the MeNBs in the cooperation set.
   b. If the received CS throughput is equal to its own throughput (or the current), and the CS ID is smaller than its own ID (or the current):
      i. The current CS ID will become the received CS ID.
      ii. The recipient forwards the new CS information to the MeNBs in the cooperation set.
   c. If the received CS throughput and ID are equal to the current CS throughput and ID, the CS elected. Stop.
   d. Otherwise, the recipient MeNB declares itself as the new CS and sends the CS information to the other MeNBs in the CoMP cooperation set.
6. If the cell throughput or cooperating set change, go back to step 3.

3.2. Coordination station election algorithm for DCEC-HetNets in heterogeneous cellular networks

Dense heterogeneous networks are considered as a promising technology to cope with the demand of data traffic and providing services to a massive number of users in wireless cellular networks. However, the coexistence of small cells and macro cells, and the proximity of the access points increase interference, especially for the UEs at the edge of small cells and macro cells. This interference causes significant performance degradation of the UEs [29,52]. As discussed earlier, CoMP can mitigate interference and improve the performance of the network. Here, we show an extended DCEC control architecture for heterogeneous cellular networks called DCEC-HetNet [21]. In order to select a coordination station (CS) dynamically within the DCEC-HetNet, we use the following algorithm:

1. UE_i estimates the CSI and sends it to the serving eNB_i ($MeNB_i$, $PeNB_i$ or RRH_i).
2. Serving eNB_i ($MeNB_i$, $PeNB_i$ or RRH_i) receives the CSI Feedback from the UE_i.
3. If an RRH_i receives the CSI feedback from a UE_i,
   a. RRH_i forwards the CSI feedback to the MeNB/BBU it is connected to.
   b. The MeNB/BBU calculates the CoMP cooperating set.
      Else if serving MeNB/PeNB receives the CSI Feedback
   c. MeNB/PeNB calculates the CoMP cooperating set.
4. If a CoMP cooperating set contains more than one MeNBs/PeNBs, the serving MeNB/PeNB in the CoMP set declares itself as a CS.
5. The declared CS sends a CS-Declaration message to other MeNBs/PeNBs in the set (containing the ID of the sender, the ID of the CS, and the cell throughput of the CS)
6. After receiving the message, other MeNBs/PeNBs in the cooperation set compare their throughput with the received CS throughput.
   a. If the received CS throughput is higher than the recipient's throughput (or the current):
      i. The CS ID will change to the received ID.
      ii. The recipient then forwards the new CS information to the MeNBs/PeNBs in the cooperation set.
   b. If the received CS throughput is equal to its own throughput (or the current), and the CS ID is smaller than its own ID (or the current):
      i. The current CS ID will become the received CS ID.

Table 1
Subband size according to system bandwidth for subband level feedback.

System Bandwidth (N_{RB}^{SB})	Number of RBs in a Subband (N_{RB}^{sband})
6 - 7	NA
8 - 10	4
11 - 26	4
27 - 63	6
64 - 110	8

      ii. The recipient then forwards the new CS information to the MeNBs/PeNBs in the cooperation set.
   c. If the received CS throughput and ID are equal to the current CS throughput and ID, the CS has been elected. Stop.
   d. Otherwise, the recipient MeNB/PeNB declares itself as the new CS and sends a CS information to the other MeNBs/PeNBs in the CoMP cooperation set.
7. If the cell throughput or cooperating set change, go back to step 4.

4. CSI feedback schemes and overhead modeling

The CSI feedback reflects the recommended rank indicator (RI), a precoding matrix indicator (PMI), and channel quality indicator (CQI). The RI is the preferred transmission rank of a number of usable data streams available for CoMP transmission. The received PMI indicates which precoding matrix should be employed for downlink transmission to an eNB. The CQI reflects the channel quality corresponding to the reported PMI [53,12].

Four widely recommended CSI feedback schemes are wideband, subband, best-M and full feedback [54–56]. In this section, we derived the CSI feedback overhead model for all of the four feedback schemes based on the 3GPP specification and other research works [54–56]. We considered all the three components (CQI, PMI and RI) of CSI feedback message for deriving feedback overhead model.

- Wideband: In wideband scheme, each UE transmits one single 4-bit CQI value describing the channel quality for all of the PRBs in the bandwidth in every reported CSI. The CQI feedback overhead in this approach is as follows [55].

$$O_{fb_{CQI-WB}} = 2(4\ N_{UE}) \tag{1}$$

Therefore, from Eq. (1) we can derive the CSI feedback overhead model as shown in Eq. (2).

$$O_{fb_{CSI-WB}} = 2(4\ N_{UE})\ N_{T_X} + Nb_{RI} + Nb_{PMI} \tag{2}$$

Where, N_{T_X} is the number of transmit antenna, N_{UE} is the number of UEs served in CoMP operation, Nb_{RI} is the bit used for rank indicator (RI) and Nb_{PMI} is the allocated bits for PMI reporting in each CSI message.

- Subband level: The bandwidth is divided into N_{sband} subbands. The number of consecutive resource blocks in a subband is dependant on bandwidth as shown in Table 1 [54]. In this case, each UE feeds back to the base station one 4 bits wideband CQI and 2 bits differential CQI for each subband. The CQI feedback overhead is defined in [55] as follows.

$$O_{fb_{CQI-SB}} = 2(4 + 2\ N_{sband})\ N_{UE} \tag{3}$$

Therefore, the overhead model for the CSI feedback can be derived from Eq. (3), considering the RI and the PMI and shown in Eq. (4).

$$O_{fb_{CSI-SB}} = 2(4 + 2\ N_{sband})\ N_{UE}\ N_{T_X} + Nb_{RI} + Nb_{PMI} \tag{4}$$

Where, N_{sband} is the number of subbands in the system bandwidth.

Table 2
Subband size and corresponding selected number of subbands according to the system bandwidth.

System Bandwidth (N_{RB}^{SB})	Number of RBs in a Subband (N_{RB}^{sband})	Selected number of Subbands (M)
6 - 7	NA	NA
8 - 10	4	1
11 - 26	4	3
27 - 63	6	5
64 - 110	8	6

Table 3
Number of bits in RI according to the antenna ports.

	Antenna ports		
	2	4	8/12/16/20/24/28/32
Number of bits in rank indicator (RI)	1	2	3

- UE selected Best-M: Each UE selects M preferred subbands of equal size N_{RB}^{sband} as shown in Table 2 [56]. In UE selected Best-M scheme, each user feeds back one 4 bits wideband CQI and 2 bits differential CQI to the serving eNB. The 2 bits differential CQI reflects the channel quality only the selected M subbands. In this scheme, UE also report the position of these subbands in the bandwidth. The Eq. (5) shows the CQI overhead for this feedback approach [55].

$$O_{fb_{CQI-BM}} = 2\left(4 + 2 + \left\lceil \log_2 \binom{N_{RB}^{SB}}{M} \right\rceil\right) N_{UE} \tag{5}$$

From Eq. (5) we can derive the Eq. (6) showing the CSI feedback overhead for this feedback scheme.

$$O_{fb_{CSI-BM}} = 2\left(4 + 2 + \left\lceil \log_2 \binom{N_{RB}^{SB}}{M} \right\rceil\right) N_{UE}\, N_{T_X} + Nb_{RI} + Nb_{PMI} \tag{6}$$

Where, N_{RB}^{SB} is the number of resource blocks in system bandwidth.

- Full Feedback: In this scheme, each UE reports a 4-bit wideband CQI value and a 2-bit differential CQI for each RB in the system bandwidth. The CQI feedback overhead is modeled as follows [55].

$$O_{fb_{CQI-F}} = 2\left(4 + 2\, N_{RB}^{SB}\right) N_{UE} \tag{7}$$

Therefore, CSI feedback overhead for this scheme can be derived from Eq. (7) and presented as Eq. (8).

$$O_{fb_{CSI-F}} = 2\left(4 + 2\, N_{RB}^{SB}\right) N_{UE}\, N_{T_X} + Nb_{RI} + Nb_{PMI} \tag{8}$$

The number of bits used in reporting rank indicator (RI) is shown in Table 3. Finally, the number of bits used to repost PMI is 2 bits and 4 bits for 2 and 4 transmit antenna ports respectively [56,48,54].

In the next section we presented simulation scenarios and results to analyze performance of the DCEC CoMP coordination architecture.

5. Simulation scenarios and results

In order to study the coordination architectures of CoMP combined with DCEC and DCEC-HetNet, we run a number of simulation scenarios using the different architectures suggested by 3GPP [22]. These suggested architectures are presented in Fig. 6, which shows simplified version of the sample scenarios. Fig. 6(a) and (b) shows homogeneous networks with 3 macro cells and 19 macrocells respectively. Fig. 6(c) and (d) shows heterogeneous networks with 3 macro cells and 3 RRHs, and 7 macrocells and 19 RRHs respectively. Fig. 6(e) is more dense networks with 7 macro cells and 10 picocells in each of the macro cells. The macro eNBs and the pico eNBs are connected using X2 link. The RRHs connect to the MeNBs through fiber optic [22]. The numbers of UEs varies in different scenarios and discussed in detail later.

To evaluate the potential of the DCEC and DCEC-HetNet coordination architectures, we ran a series of simulations based on the scenarios discussed in Fig. 6, using the initial conditions summarized in Table 4 [18,57,58].

In our simulation scenarios, we consider homogeneous and heterogeneous networks in an urban area. The transmit power for a MeNB is 43 dBm, PeNB is 30 dBm and the RRH is 30 dBm, as suggested in [21,57,59]. The received signal power at each UE is calculated based on the following formula [57]:

$$P_r = P_t - Max\left(L_{path} - G_t - G_r,\ MCL\right) \tag{9}$$

Where P_r is the received signal power, P_t is the transmitted signal power of the BS, L_{path} is the path loss, G_t is the transmitting antenna gain and G_r is the receiver antenna gain. The Minimum coupling loss (MCL) is considered to be 70 dB [57]. L_{path} is calculated as follows:

$$L_{path} = L + LogF \tag{10}$$

Where L is calculated based on the following formula as suggested by 3GPP in [57]:

$$L = 40(1 - 4 \times 10^{-3} B_h) \log_{10}(d) - 18 \log_{10}(B_h) + 21 \log_{10}(f) + 80 dB \tag{11}$$

Here, B_h is the base station height, which we considered to be 15 m, d is the distance between UE and eNB and f is the carrier frequency.

The UEs calculate the received power based on the above formula, they generate a CSI feedback message, and they send it to the eNBs. In our simulation, the MeNBs and PeNBs generate the cell throughput to select the CS at random. Based on the literature in this area, we considered the CoMP threshold as 6 dB [46–48].

Fig. 7 shows the number of control messages related to the CoMP download transmission that traveled from the UEs to the CS/MeNBs and the backhaul in specific time intervals, for all the three coordination architectures. In this figure, the three bars in every group represent the three architectures in the following order: DCEC, centralized and distributed. In this case we considered simulation scenarios with three macro cells as shown in Fig. 6(a) and (c).

The darker part of each bar in the figure shows the number of CSI Feedback messages which traveled from UE to MeNB or RRH. The lighter part shows the CSI feedback forwards from MeNB to MeNB, from MeNB to CU and the overhead related to the election algorithm. Each bar represents 10 ms of simulated time. In this scenario, the UEs send the CSI feedback to their serving MeNB/RRH or CS every 10 ms. The results of the simulations show that in the transient period when we establish CoMP, DCEC needs more control messages over the backhaul because of the election of the CS. After the CS has been elected there are no control messages transmitted into the backhaul as CS worked as a scheduler for the UE. Therefore, only the CSI feedback from the UE to the CS is required. As it is seen in Fig. 7(a), no additional control messages are transmitted from MeNB to MeNB within the 30 to 80 ms timeframe in
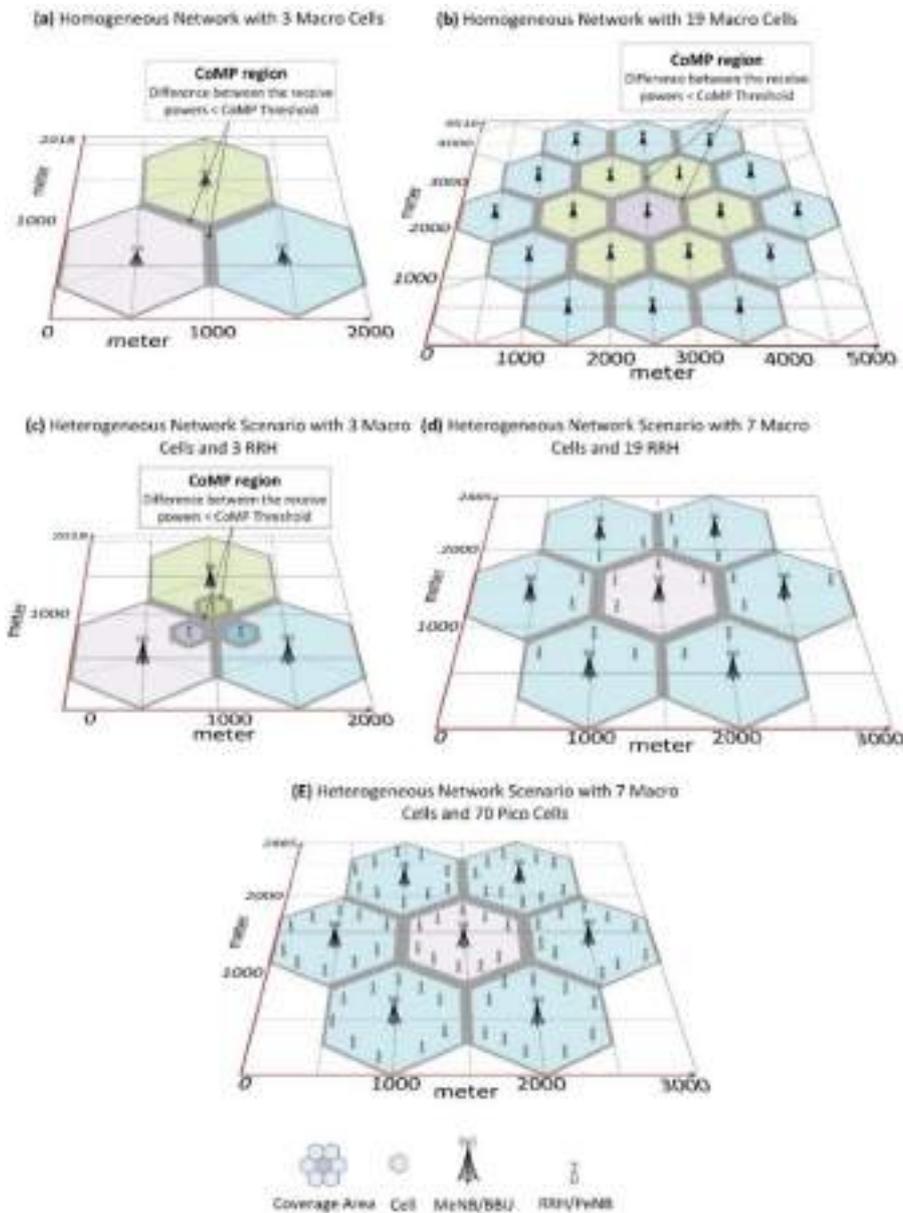
Fig. 6. Network architectures of simulation scenarios.

Table 4

Simulation assumptions.

| Parameters	Values
Number of macro MeNB	3 and 19 (Homogeneous)
	3 and 7 (Heterogeneous)
Number of RRHs in HetNets	3 and 19
Number of PeNBs in HetNets	70
Density of active UEs in Macro only networks	$2/km^2$, $4/km^2$, $6.5/km^2$ and $9/km^2$
Density of active UEs in HetNets	$6/km^2$, $11.5/km^2$, $17/km^2$ and $23/km^2$
UE Spatial Distribution	Uniform random distribution in the CoMP area
UE arrival and leave	Uniform random and Poisson
Frequency	2000 MHz
eNB Transmit Power	MeNB: 43 dBm, PeNB: 30 dBm and RRH: 30 dBm
Macro Cell Radius	500 m
Cell Throughput	Uniform: randomly generated
CSI Feedback periodicity	5 ms
CoMP Threshold	6 dB
ISD	MeNB to PeNB > 100 m
	PeNB to PeNB > 50 m
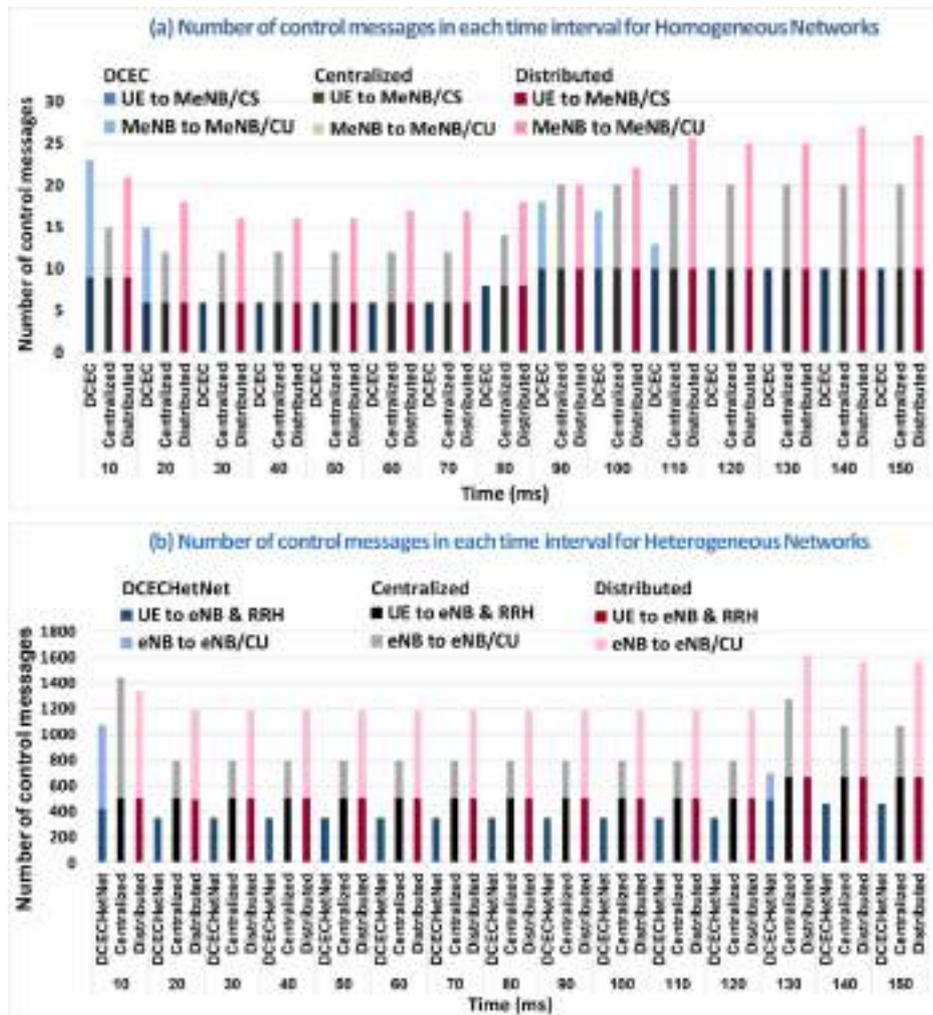
Fig. 7. Number of control messages at different time intervals for DCEC, Centralized and Distributed architectures: messages over the backhaul and radio links.

DCEC. From 80 ms to 110 ms, there are several new UEs joining the CoMP transmission, which results in additional control messages transmitted from the UEs to the MeNBs, as well as from MeNB to MeNB (to elect the CS). Likewise, from 120 ms, there are no additional control messages transmitted through the X2 interface in DCEC (since the CS has been selected). On the other hand, in the two other conventional architectures (centralized and distributed) the CSI feedback needs to be forwarded over the backhaul every time. Fig. 7(b) shows the same idea for heterogeneous networks in each 10 ms time intervals for all the three architectures with 200 UEs in CoMP cooperation. As clearly seen in Fig. 7(b), no additional control packets transmitted from eNB to eNB within the 20 ms to 120 ms (inclusive) timeframe in DCEC-HetNet. In the 130–140 ms timeframe, several new UEs join the CoMP which results in some additional control packets being transmitted through the backhaul to elect the CS for the new UEs. Again, from time 140 ms, there are no additional control packets required since the CS election has been completed for the newly joined UEs. On the other hand, the other two conventional architectures need the CSI feedback to be forwarded over the backhaul every time. The X2 latency is 10–20 ms [40,41]. Therefore, according to the simulation results (Fig. 7), DCEC reduces the CSI feedback latency and number of CSI feedback messages (signaling overhead) compared to the other two control architectures.

Fig. 8 shows the number of control messages related to the CoMP download transmission that traveled into the network for all the three coordination architectures. Here we considered, a simulation scenario with 19 cells homogeneous network as shown in Fig. 6(b) with different density of active UEs within the CoMP operation. The UEs were set to join CoMP based on a Poisson distribution within a 12-hour period (6 AM to 6 PM) with the peak rate at 10 AM, as suggested in [60]. As stated earlier, the factors that affect the download and upload performance resulting in a change in cell edge user experience are the signaling overhead and latency in CoMP networks. The results are further analyzed for the comparison of the number of CSI feedback messages and delay. Fig. 8 shows that using DCEC, the number of feedback messages can be reduced significantly, resulting in better throughput. The results are obtained by conducting 30 simulation runs for each scenario and considering a 95% confidence interval.

As seen in Fig. 8, DCEC reduces the CSI feedback messages in the network about 50%. This is because after a base station is elected to act as the coordination station (CS), eNBs do not need to exchange CSI feedback messages among them. This reduces the signaling load and the possibility of outdated CSI messages that eventually increase the upload and download rate of CoMP operation.

For DCEC-HetNet, in the following results we considered the simulation scenario with 7 macro cells and 19 small cells, as shown in Fig. 6(d), with a different density of active UEs. The UEs join and leave to the CoMP operation randomly. The CSI feedback periodicity is considered 5 ms. The results are collected and ana-
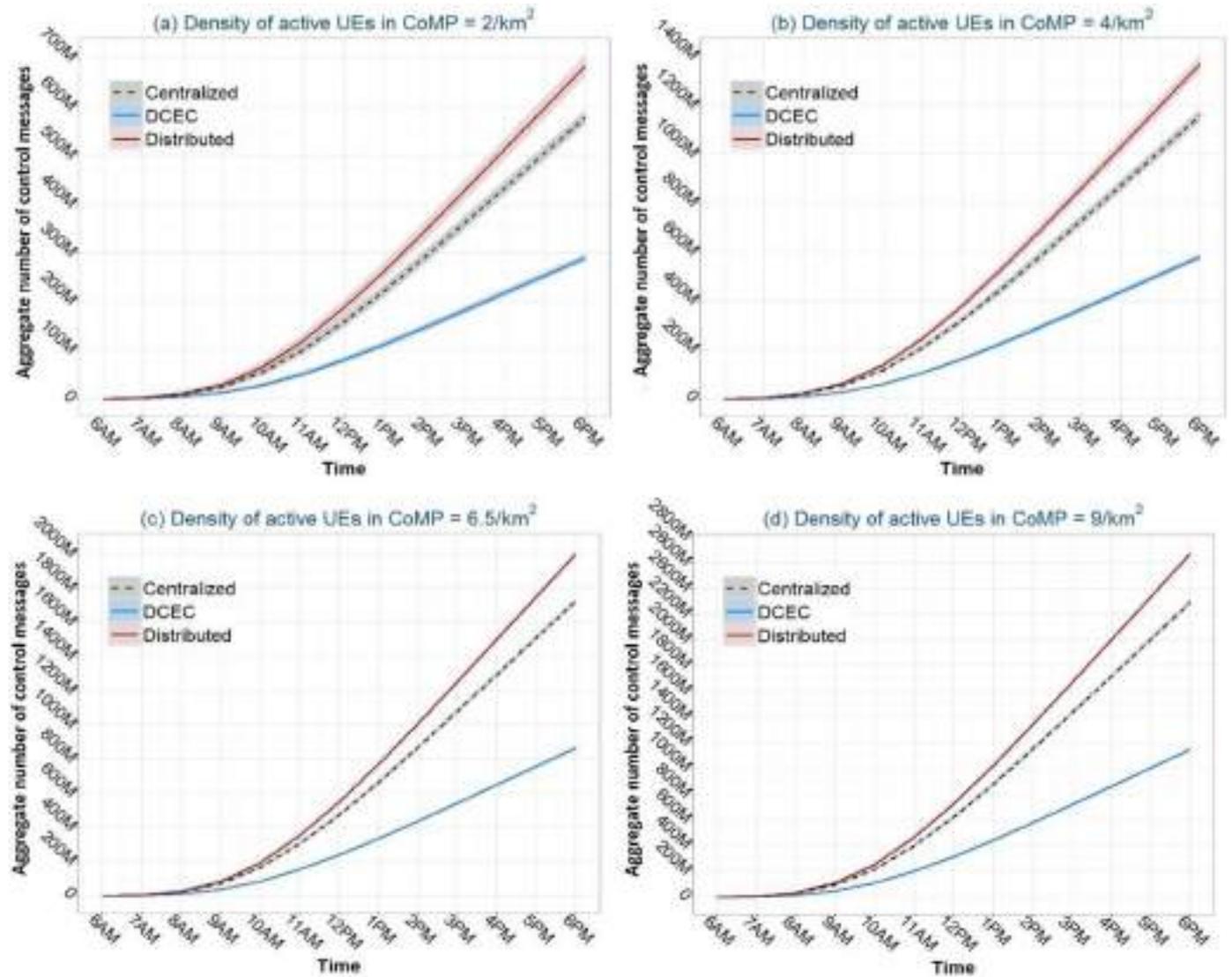
Fig. 8. Cumulative number of messages for Centralized, DCEC and Distributed based on the density of the active UEs into CoMP in macro only networks.

lyzed for the comparison of the number of control message required for each of the three control architectures. Fig. 9 demonstrates that by the use of DCEC-HetNet, the number of feedback messages can significantly be reduced in the network resulting in better throughput. This is because after an eNB is elected to act as the CS, the CSI feedback message does not need to exchange among the cooperating eNBs. This result shows that DCEC-HetNet also reduces the signaling load and the possibility of outdated CSI messages on the heterogeneous networks that eventually will improve the system performance.

We increase the density of the networks in heterogeneous simulation scenarios including 7 macrocells and 70 picocells (10 picocells in each macrocell) as shown in Fig. 6(e) and different density $(6/km^2$, $11.5/km^2$ and $23/km^2)$ of active UEs in the cell edge area to observe how the DCEC-HetNet works in dense heterogeneous networks. The CSI feedback periodicity is considered 5 ms and we use simulation time of 30 min. The UEs join and leave the CoMP operation randomly in the simulation time. Fig. 10 demonstrates that by employing the DCEC-HetNet, the number of feedback messages significantly reduced in the dense heterogeneous cellular networks as well. This once again confirm that DCEC-HetNet reduces the signaling load on the cooperative cellular networks.

For further study, in Fig. 11(a) we show the total amount of overhead in GB for 100 UEs in 30 min simulation time with respect to different CSI feedback schemes suggested by 3GPP and other recent research works as we discussed in Section 4. In this case, we used the scenario as shown in Fig. 6(e) and considered 100 UEs served in CoMP operation into the entire networks. For calculating the overhead, we used the Eqs. (2), (4), (6) and (8) derived in Section 4 for four different CSI feedback schemes (wideband, subband level, UE selected best-M and full feedback). In every scheme DCEC-HetNet reduces the overhead significantly. In Fig. 11(b), we present the signaling overhead per second with respect to different feedback schemes. Fig. 11 clearly shows DCEC-HetNet also reduce the signaling overhead significantly with respect to the number of bits in every scheme of the CSI feedback that eventually will save the system bandwidth. This once again prove the improvement of DCEC on top of the two other coordination architectures.

Fig. 12 shows the cumulative number of control messages transmitted up to a certain time for each of the architectures in the logarithmic scale. DCEC architecture is represented by three instances to see how the CS changes affect the number of control messages transmitted. In the first case, we assume that the throughput is constant, that is, the CS does not change throughout
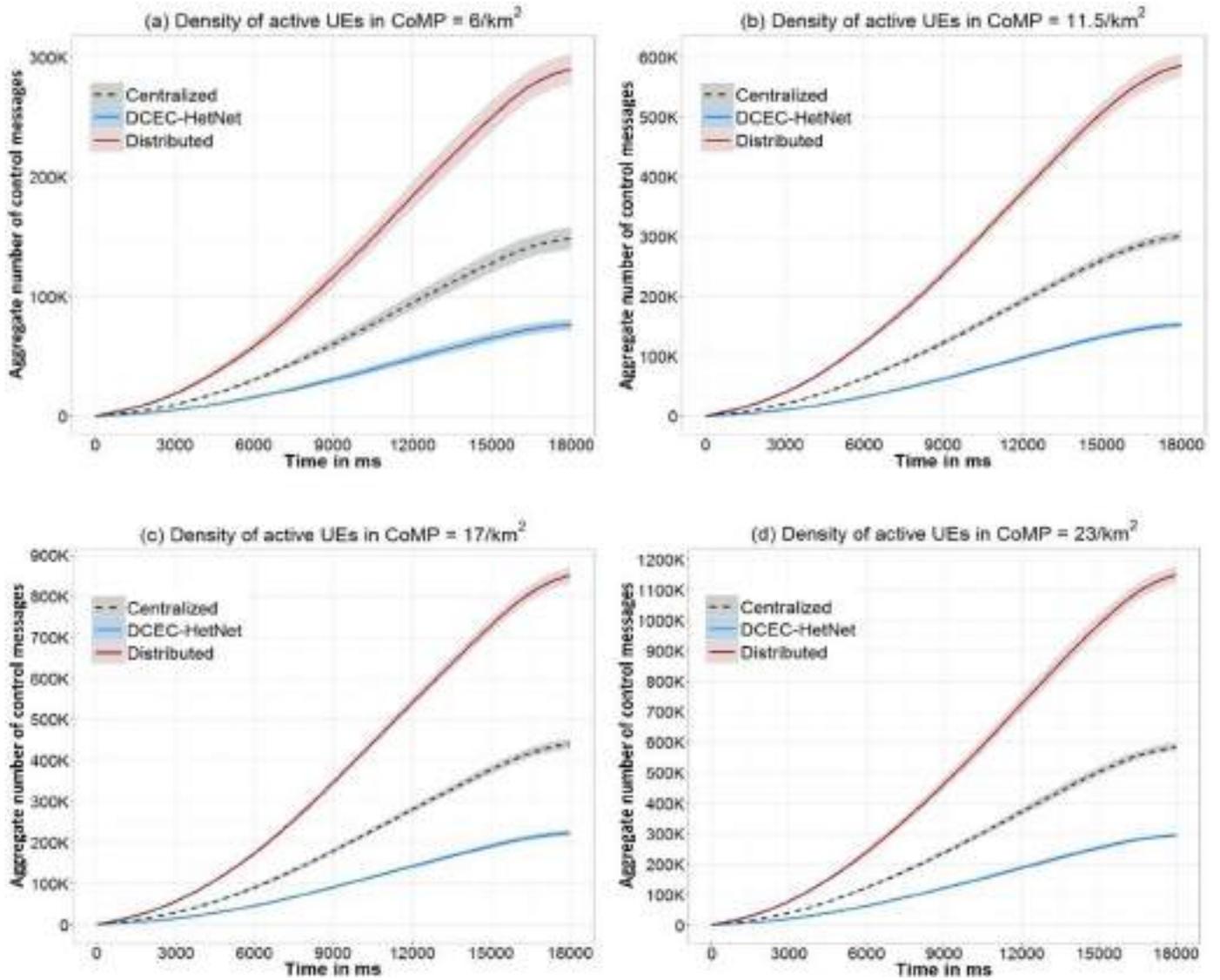
Fig. 9. Aggregate number of control messages for Centralized, DCEC-HetNet and Distributed based on the density of the active UEs into CoMP cooperation in heterogeneous networks.
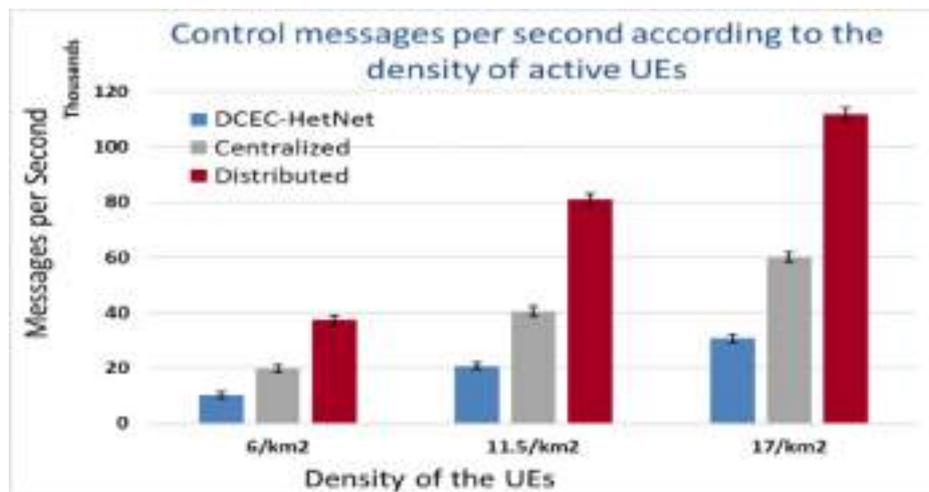

Fig. 10. Number of control messages per second for DCEC-HetNet, Centralized and Distributed CoMP coordination architecture based on the density of the active UEs into in heterogeneous networks.
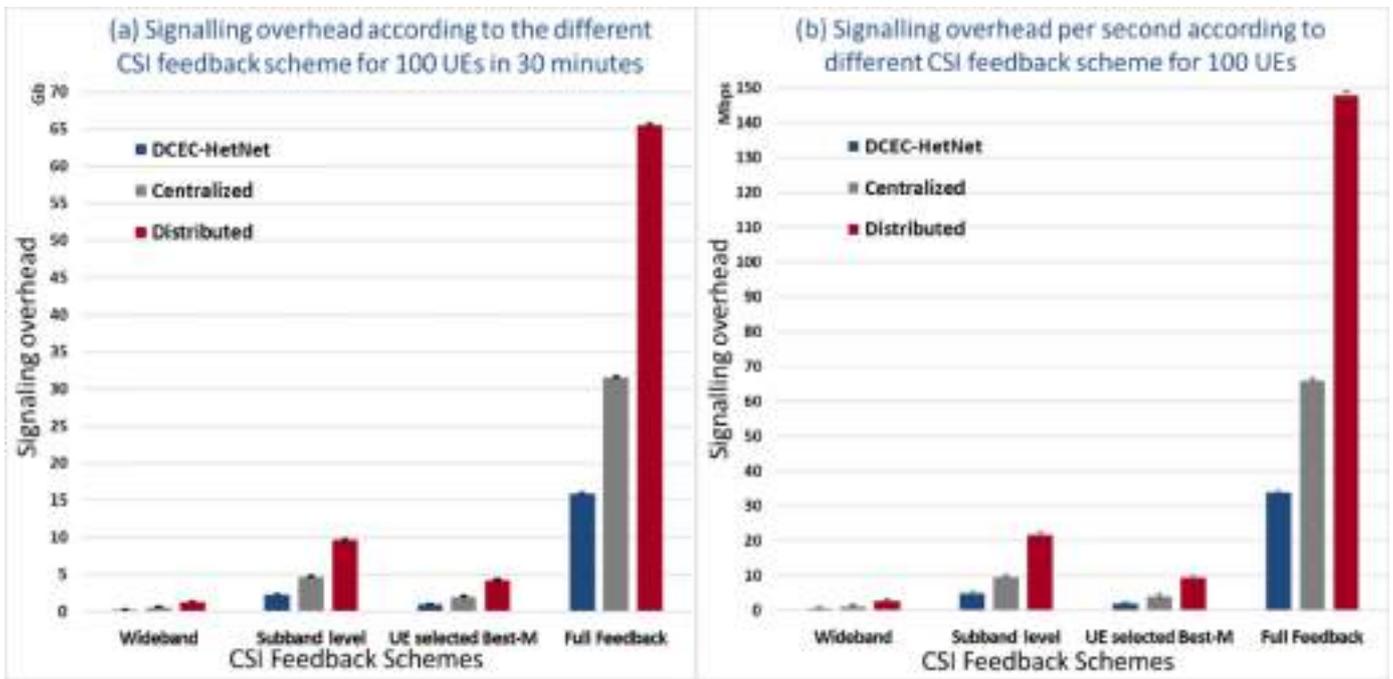
Fig. 11. Signaling overhead in DCEC-HetNet, Centralized and Distributed CoMP coordination architecture with respect to different CSI feedback schemes for 100 UEs.
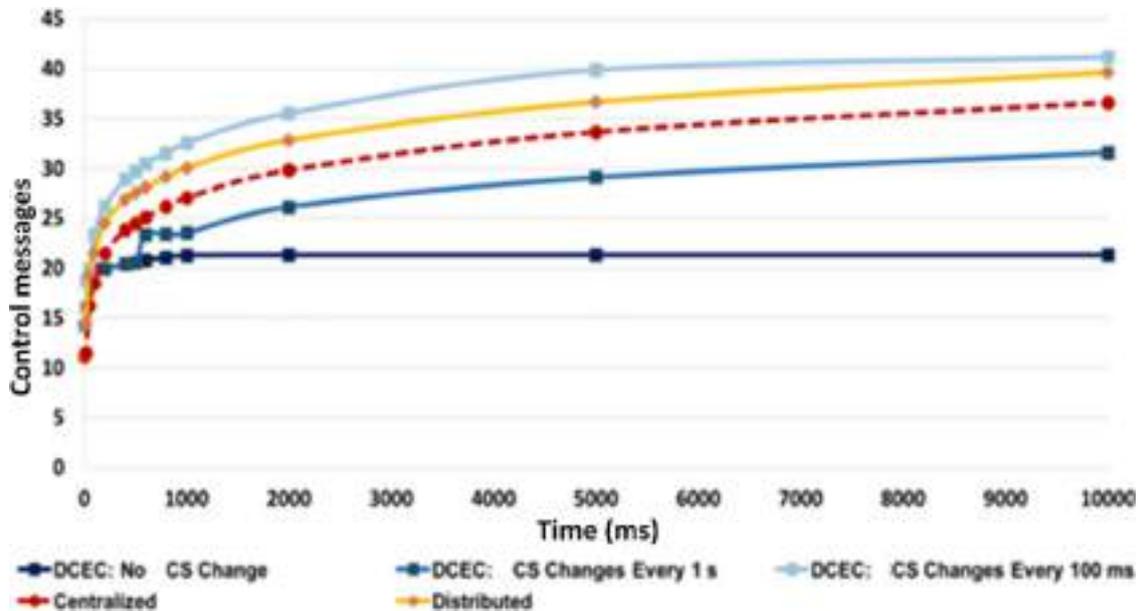

Fig. 12. Cumulative control messages for DCEC without CCS change, DCEC with CCS change every 1 s/100 ms, Centralized, and Distributed Architectures.

the simulation time. In the second and third cases, the CS is set to change every 100 ms and every 1 s respectively. As we can see, DCEC with no CS changes or with changes every 1 s outperform the centralized and distributed architectures. If the CS change occurs very rapidly, for example, every 100 ms, DCEC will be less efficient than the traditional approaches. Therefore, if the rate of the CS changes is very high, DCEC will perform worse than the centralized and distributed architectures. In practice, the CS change does not occur that frequently for most of the UEs since the maximum movement speed of a UE suggested by the 3GPP release 11 and 14 for CoMP deployment is 3 km/h [61,10].

In most practical systems, the CSI feedback latency consists of processing time, transmission time and waiting time for the scheduler [33]. Here, we use the feedback delay as the total time be-

tween measuring the CSI at the UE and receiving at the scheduler. The increase in CSI feedback messages might result in higher delay. Here, we measured the feedback delay for every CSI feedback sent by the UE and received by the scheduler. To find the average feedback delay of the system, we calculated the average feedback delay of all the UEs for 30 separate simulation runs to minimize anomalies. Fig. 13 shows the average CSI feedback delay of the entire system for a different number of UEs.

The above figure shows that DCEC imposes the least amount of average feedback delay on the network while the centralized approach imposes the most. It can be confirmed once again that the DCEC approach is less sensitive to the increase in the number of UEs in the network. This allows for DCEC to be a good fit for both crowded and uncrowded areas.
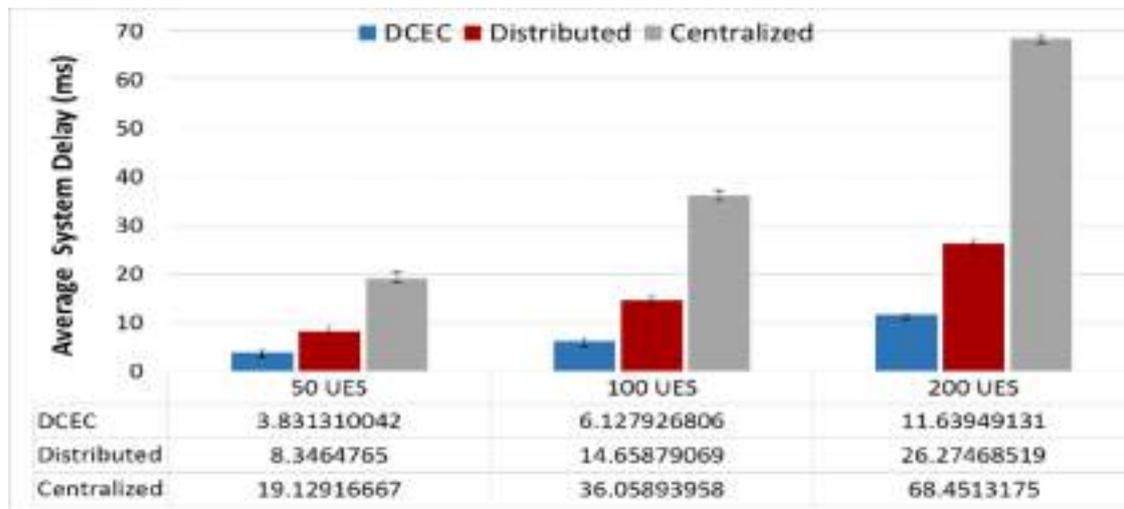
Fig. 13. Average system delay for 50, 100, and 200 UEs.

According to the simulation results, shown in Figs. 7–13 we can see that DCEC has the potential to reduce the signaling overhead as well as the CSI feedback latency without changing the periodicity of the CSI feedback. The reduction of the CSI feedback overhead and latency eventually improve the network throughput [62,63].

4. Conclusion

The main goal of the CoMP approach is to improve the throughput of the network, especially for the cell edge users. However, the two standard architectures of CoMP (centralized and distributed) face some challenges such as feedback latency, signaling overhead and infrastructural overhead. The promising gain of CoMP largely depends on these overhead and latency. In this work, we presented a novel algorithm named DCEC for CoMP operation in homogeneous cellular networks to reduce the feedback latency and the signaling overhead so that the cell edge throughput of the network could be improved. The algorithm also extended for heterogeneous networks named DCEC-HetNet. The simulation results show that the DCEC coordination architecture for CoMP reduce the signaling overhead about 48% compare to centralized architecture and about 76% compare to distributed architecture in case of heterogeneous networks. The DCEC also reduce the CSI feedback latency significantly compared to two other standard CoMP approaches as shown in the simulation result section. This reduction of signaling overhead and feedback latency eventually will increase the network performance. Given that DCEC does not need any additional hardware for implementation, switching to DCEC could decrease the signaling load and feedback latency, and improve the network throughput at minimal cost.

Declaration of Competing Interest

The authors declare that they have no known competing financial interests or personal relationships that could have appeared to influence the work reported in this paper.

References

[1] CISCO, Cisco visual networking index: Forecast and methodology, 2016–2021, CISCO, 2017.
[2] Ericsson, Ericsson mobility report, 2016. [Online]. Available: http://www.ericsson.com/res/docs/2015/mobility-report/ericsson-mobility-report-nov-2015.pdf. [Accessed 26 March 2016].
[3] M.H. Alsharif, R. Nordin, Evolution towards fifth generation (5G) wireless networks: current trends and challenges in the deployment of millimetre wave, massive MIMO, and small cells, Telecommun. Syst. 64 (4) (2016) 617–637.
[4] M. Agiwal, R. Abhishek, S. Navrati, Next generation 5G wireless networks: a comprehensive survey, IEEE Commun. Surv. Tutor. 18 (3) (2016) 1617–1655.
[5] Qualcomm, 1000x Data challenge, 2014. [Online]. Available: https://www.qualcomm.com/invention/1000x/tools. [Accessed 15 august 2017].
[6] J.G. Andrews, Z. Xinchen, D.D. Gregory, K.G. Abhishek, Are we approaching the fundamental limits of wireless network densification? IEEE Commun. Mag. 54 (10) (2016) 184–190.
[7] A. Gotsis, S. Stelios, A. Angeliki, UltraDense networks: the new wireless frontier for enabling 5G access, IEEE Veh. Technol. Mag. 11 (2) (2016) 71–78.
[8] M. Liu, T. Yinglei, S. Mei, Performance analysis of comp in ultra-dense networks with limited backhaul capacity, Wirel. Pers. Commun. 91 (1) (2016) 51–77.
[9] S. Bassoy, F. Hasan, I. Muhammad A., I. Ali, Coordinated multi-point clustering schemes: a survey, IEEE Commun. Surv. Tutor. 19 (2) (2017) 743–764.
[10] 3GPP, 3GPP TR 36.741 V14: Study on further enhancements to coordinated multi-point (CoMP) operation for ltE, 23 March 2017. [Online]. Available: http://www.3gpp.org/DynaReport/36-series.htm. [Accessed 18 August 2017].
[11] S. Chen, Z. Tianyu, C. Hsiao-Hwa, L. Zhiping, M. Weixiao, Performance analysis of downlink coordinated multipoint joint transmission in ultra-dense networks, IEEE Netw. 31 (5) (2017) 106–114.
[12] M. Ding, H. Luo, Multi-Point Cooperative Communication Systems: Theory and Applications, Shanghai Jiao Tong University Press, Shanghai and Springer-Verlag, Berlin Heidelberg, 2013.
[13] B. Özbek, D.L. Ruyet, Feedback strategies for multicell systems, in: Feedback Strategies for Wireless Communication, Springer, New York, 2014, pp. 249–293.
[14] S. Sun, Q. Gao, Y. Peng, Y. Wang, L. Song, Interference management through comp in 3GPP LTE-Advanced networks, IEEE Wirel. Commun. 20 (1) (2013) 59–66.
[15] P. Marsch, G.P. Fettweis, Coordinated Multi-Point in Mobile Communications: From Theory to Practice, Cambridge University Press, 2011.
[16] A. Papadogiannis, H. Bang, D. Gesbert, E. Hardouin, Efficient selective feedback design for multicell cooperative networks, IEEE Trans. Veh. Technol. 60 (1) (2011) 196–205.
[17] A. Papadogiannis, E. Hardouin, D. Gesbert, Decentralising multicell cooperative processing: a novel robust framework, EURASIP J. Wirel. Commun. Netw. 2009 (2009) 890685 April doi:10.1155/2009/890685.
[18] I.F. Akyildiz, D.M. Gutierrez-Estevez, E.C. Reyes, The evolution to 4G cellular systems: LTE-Advanced, Phys. Commun. 3 (2010) 217–244.
[19] B.U. Kazi, G.A. Wainer, G. Boudreau and R. Casselman, Coordinated multi-point (CoMP) method and systems using a coordination station. Canada Patent P47112 US2, 2015.
[20] B.U. Kazi, M. Etemad, G. Wainer, G. Boudreau, Using elected coordination stations for csi feedback on comp downlink transmissions, in: Proceedings of the International Symposium on Performance Evaluation of Computer and Telecommunication Systems, Montreal, Canada, 2016.
[21] B.U. Kazi, M. Etemad, G. Wainer, G. Boudreau, Signaling overhead and feedback delay reduction in heterogeneous multicell cooperative networks, in: Proceedings of the International Symposium on Performance Evaluation of Computer and Telecommunication Systems, Montreal, Canada, 2016.
[22] 3GPP, 3GPP TR 36.819 version 11.2.0: Coordinated multi-point operation for lte physical layer aspects, 09 2013. [Online]. Available: http://www.3gpp.org/DynaReport/36-series.htm. [Accessed September 2016].
[23] M. Peng, Y. Li, Z. Zhao, C. Wang, System architecture and key technologies for 5G heterogeneous cloud radio access networks, IEEE Netw. 29 (2) (2015) 6–14.
[24] C.-.X. Wang, F. Haider, X. Gao, X.-.H. You, Y. Yang, D. Yuan, H. Aggoune, H. Haas, S. Fletcher, E. Hepsaydir, Cellular architecture and key technologies for 5G wireless communication networks, IEEE Commun. Mag. 52 (2) (2014) 122–130.
[25] 3GPP, 3GPP TR 36.842 V12.0: Study on small cell enhancements for e-utra and E-UTRAN; higher layer aspects, January 2014. [Online]. Available: http://www.3gpp.org/DynaReport/36-series.htm. [Accessed July 2016].

[26] V. Jungnickel, K. Manolakis, W. Zirwas, B. Panzner, V. Braun, M. Lossow, M. Sternad, R. Apelfröjd, a.T. Svensson, The role of small cells, coordinated multipoint, and massive mimo in 5G, Commun. Mag. 52 (5) (2014) 44–51.

[27] S. Chen, F. Qin, B. Hu, X. Li, J. Liu, C. Shanzhi, Ultra-dense network architecture and technologies for 5G, in 5G Mobile communications, Spring. Inter. Publ. (2017) 403–429.

[28] D. Lopez-Perez, I. Guvenc, G. d. l. Roche, M. Kountouris, T.Q.S. Quek, J. Zhang, Enhanced intercell interference coordination challenges in heterogeneous networks, IEEE Wirel. Commun. 18 (3) (2011) 22–30.

[29] H. Ishii, K. Yoshihisa, T. Hideaki, A novel architecture for LTE-B: C−plane/U-plane split and phantom cell concept, in: Proceedings of the IEEE Globecom Workshops, California, USA, 2012.

[30] J. Lee, Y. Kim, H. Lee, B.L. Ng, D. Mazzarese, J. Liu, W. Xiao, Y. Zhou, Coordinated multipoint transmission and reception in LTE-Advanced systems, IEEE Commun. Mag. 50 (11) (2012) 44–50.

[31] P. Liu, Z. Tao, N. Sathya, K. Thanasis, S.P. Shivendra, CoopMAC: a cooperative mac for wireless LANs, IEEE J. Sel. Areas Commun. 25 (2) (2007) 340–354.

[32] T. Jamal, M. Paulo, Z. André, Analysis of hybrid relaying in cooperative WLAN, in: Proceedings of the IFIP Wireless Days (WD), Valencia, Spain, 2013.

[33] S. Brueck, L. Zhao, J. Giese, A. Amin, Centralized scheduling for joint transmission coordinated multi-point in LTE-Advanced, in: Proceedings of the International ITG Workshop on Smart Antennas (WSA), Bremen, 2010.

[34] T. Okamawari, H. Hayashi, T. Fujii, A proposal on network control architecture for comp jt with ip network between eNBs, in: Proceedings of the IEE Vehicular Technology Conference, Yakohama, 2012.

[35] Y. Gao, Y. Li, H. Yu, S. Gao, Performance of dynamic comp cell selection in 3GPP lte system level simulation, Proceeding of the IEEE Third International Conference On Communication Software and Networks, Xi'an, 2011.

[36] Y. Gao, Y. Li, H. Yu, a.S. Gao, Performance analysis of dynamic comp cell selection in LTE-advanced heterogeneous networks scenario, Proceeding of the International Conference on Uncertainty Reasoning and Knowledge Engineering (URKE), Bali, Indonesia, 2011.

[37] S. Geirhofer, a.P. Gaal, Coordinated multi point transmission in 3GPP lte heterogeneous networks, Proceeding of the Globecom Workshops (GC Wkshps), Anaheim, CA, 2012.

[38] A. Hajisami, P. Dario, Cloud-CFFR: coordinated fractional frequency reuse in cloud radio access network (C-RAN), Proceeding of the IEEE Twelfth International Conference On Mobile Ad Hoc and Sensor Systems, 2015 Dallas, TX, USA.

[39] A. Hajisami, P. Dario, Dynamic joint processing: achieving high spectral efficiency in uplink 5G cellular networks, Comput. Netw. 126 (2017) 44–56.

[40] D.H. Nguyen, L.-.N. Tho, Wireless Coordinated Multicell Systems: Architectures and Precoding Designs, Montréal, Springer, QC, Canada, 2014.

[41] C. Yang, H. Shengqian, H. Xueying, M. Andreas, How do we design comp to achieve its promised potential, IEEE Wirel. Commun. 20 (1) (2013) 67–74.

[42] B. Mielczarek, W. Krzymien, Influence of csi feedback delay on capacity of linear multi-user mimo systems, Proceeding of the IEE Wireless Communications and Networking Conference, 2007 *WCNC 2007*, Kowloon.

[43] 3GPP, 3GPP TR 36.932 V13: Scenarios and requirements for small cell enhancements for e-utra and e-utraN, 2016-01. [Online]. Available: http://www.3gpp.org/DynaReport/36-series.htm. [Accessed August 2016].

[44] B. Zeigler, H. Praehofer, T. Kim, Theory of Modeling and Simulation, Academic Press, San Diego, CA, 2000.

[45] G.A. Wainer, Discrete Event Modeling and Simulation a Practitioner's Approach, CRC Press, Taylor & Francis Group, Boca Raton, FL, 2009.

[46] G. Cili, H. Yanikomeroglu, F.R. Yu, Cell switch off technique combined with coordinated multi-point (CoMP) transmission for energy efficiency in beyond-lte cellular networks, Proceeding of the IEEE International Conference on Communications (ICC), Ottawa, ON, 2012.

[47] X. Zhang, X. Zhou, LTE-Advanced Air Interface Technology, CRC Press, 2012.

[48] A. Davydov, M. Gregory, B. Ilya, A. Papathanassiou, Evaluation of joint transmission comp in c-ran based lte-a hetnets with large coordination areas, in: Proceeding of the IEEE Globecom Workshops (GC Wkshps), IEEE, Atlanta, GA, USA, 2013, pp. 801–806. 2013.

[49] M. Liu, T. Yinglei, S. Meng, Effects of outdated csi on the coverage of comp-based ultra-dense networks, Proceeding of the IEEE Eighteenth International Workshop On Signal Processing Advances in Wireless Communications (SPAWC), Sapporo, Japan, 2017.

[50] Backhauling X2, Cambridge broadband networks, April 2011. [Online]. Available: http://cbnl.com/resources/backhauling-x2. [Accessed February 2016].

[51] Stoke, Latency considerations in lte, September 2014. [Online]. Available: http://mavenir.com/files/doc_downloads/Stoke_Documents/130-0029-001_LTELatencyConsiderations_Final.pdf. [Accessed December 2015].

[52] Y.-N.R. Li, J. Li, W. Li, Y. Xue, H. Wu., CoMP and interference coordination in heterogeneous network for LTE-advanced, in: Proceedings of the IEEE Globecom Workshops, IEEE, 2012, pp. 1107–1111. California, USA, December, 2012.

[53] S. Sun, Q. Gao, Y. Peng, Y. Wang, L. Song, Interference management through comp in 3GPP LTE-advanced networks, IEEE Wirel. Commun. 20 (1) (2013).

[54] 3GPP, 3GPP TS 36.213 V15.1.0: Evolved universal terrestrial radio access (E-UTRA), physical layer procedures (Release 15), April 2018. [Online]. Available: http://www.3gpp.org/DynaReport/36-series.htm. [Accessed 2018].

[55] A. Chiumento, C. Desset, P. Sofie, V. d. P. Liesbet, R. Lauwereins, Impact of CSI feedback strategies on lte downlink and reinforcement learning solutions for optimal allocation, IEEE Trans. Veh. Technol. 66 (1) (2017) 550–562.

[56] 3GPP, 3GPP TS36.212, V15.1.0: evolved universal terrestrial radio access (E-UTRA); multiplexing and channel coding, 4 2018. [Online]. Available: http://www.3gpp.org/DynaReport/36-series.htm. [Accessed 5 2018].

[57] 3GPP, 3GPP TR 36.942 V13.0: evolved universal terrestrial radio access (E-UTRA); radio frequency (RF) system scenarios, 01 2016. [Online]. Available: http://www.3gpp.org/DynaReport/36-series.htm. [Accessed April 2016].

[58] 3GPP, "3GPP TS 36.211 version 14.0: evolved universal terrestrial radio access (E-UTRA); physical channels and modulation," 09 2016. [Online]. Available: http://www.3gpp.org/DynaReport/36-series.htm. [Accessed February 2016].

[59] B. Mondal, E. Visotsky, T. Thomas, X. Wang, A. Ghosh, Performance of downlink comp in lte under practical constraints, Proceeding of the IEEE 23rd International Symposium On Personal Indoor and Mobile Radio Communications (PIMRC), Sydney, NSW, 2012.

[60] SalesForce, Mobile behavior report, SalesForce, 2014.

[61] 3GPP, 3GPP TR 36.819 version 11.2.0, 09 2013. [Online]. Available: http://www.3gpp.org/DynaReport/36-series.htm. [Accessed September 2015].

[62] B. Mielczarek, W. Krzymien, Influence of csi feedback delay on capacity of linear multi-user mimo systems, in: Proceedings of the IEE Wireless Communications and Networking Conference, Kowloon, 2007.

[63] L. Shi, H. Zhirui, Z. Tiankui, Z. Zeng, Performance analysis of delayed limited feedback based on per-cell codebook in comp systems, in: Proceedings of the Wireless Communications and Networking Conference (WCNC), IEEE, New Orleans, LA, USA, 2015.

Baha Uddin Kazi received a Ph.D. in the Department of Systems and Computer Engineering at Carleton University. He received his MASc in Computer Networks from Ryerson University. He is serving as a member of the technical committee of several international conferences. His research interests focus on performance engineering, modeling and simulation, wireless cellular networks and network protocols.

Gabriel A. Wainer, FSCS, SMIEEE, is Professor and Associate Chair for Graduate Studies, Department of Systems and Computer Engineering (Carleton University). He held visiting positions at the University of Arizona; LSIS (CNRS), Université Paul Cézanne, University of Nice, INRIA Sophia- Antipolis, Université Bordeaux (France); UCM, UPC (Spain), and others. He is the author of three books and over 350 research articles; he helped organizing over 100 conferences, being one of the founders of the Symposium on Theory of Modeling and Simulation, SIMUTools and SimAUD. Prof. Wainer is Special Issues Editor of SIMULATION, member of the Editorial Board of IEEE/AIP CISE, Wireless Networks (Elsevier), and others. He received the IBM Eclipse Innovation Award, the First Bernard P. Zeigler DEVS Modeling and Simulation Award, the SCS Outstanding Professional Award (2011), the SCS Distinguished Professional Award (2013), the SCS Distinguished Service Award (2015) and various Best Paper awards. He is a Fellow of SCS.